Experimental Analysis and Implementation of Redundant Thrusters for Underwater Robots

A. Hanai, K. Rosa, S.K. Choi
Marine Autonomous Systems Engineering, Inc.
2333 Kapiolani Boulevard, Suite 912
Honolulu, HI 96826 U.S.A.
Fax: 808-942-7033
Email: (ahanai, krosa, schoi)@maseinc.com

J. Yuh
Autonomous Systems Laboratory
Mechanical Engineering Department
University of Hawai'i at Manoa
Honolulu, HI U.S.A.
Email: jyuh@eng.hawaii.edu

***Abstract*— This paper identifies the key issues in the empirical implementation of redundant marine thrusters for two different autonomous underwater vehicles of different designs, so as to maximize the effectiveness for fine motion control. A crucial factor in the development of a precision control scheme is the thorough understanding of the system geometry. Other critical elements include the contribution of the thruster amplifier gains to the steady state response of the thrusters, and the influence of the power source on system performance. These findings are proven through experimental analysis and verification.**

I. Introduction

As the applications for underwater vehicles continue to expand in practicality and desire, there is an increasing demand for autonomy in the ocean environment. Complex mission tasks may require hovering, docking, tracking, or manipulation, which necessitates fine motion control. Such autonomous precision control can be accomplished with an understanding of the dynamics and the geometry of the vehicle and the thrusters [1–4]. A relatively small, high-performance autonomous underwater vehicle (AUV) would benefit from accurate dynamic modelling of the actuators. A larger, more massive vehicle would not be affected in any significant way by the transient properties of the thruster outputs, in which case the dynamic model would not be so beneficial. In either case, a thorough understanding of the steady state characteristics of the marine thrusters would be imperative. It is also vital to understand which of the variables have the most effect on the overall system performance.

This paper addresses the key issues in the implementation and tuning of marine thrusters. The groundwork for a steady state thruster model is completed experimentally, based on two AUVs of different design. The first is the Omni-Directional Intelligent Navigator (ODIN) [5], which is a relatively smaller-sized vehicle, and the second is the Semi-Autonomous Underwater Vehicle for Intervention Missions (SAUVIM) [6], which is a relatively large, full-ocean-depth vehicle. The critical considerations for empirical precision control application include the exploitation of the geometry, understanding and tuning of the gains for the thruster amplifiers, and recognizing the effects of the power source.

II. Thruster Configuration

A. General Vehicle Geometry

The dynamic equation of motion for an AUV can be expressed as [7]:

$$M\dot{\nu} + C(\nu)\nu + D(\nu)\nu + g(\eta) = B \tag{1}$$

where ν is linear and angular velocities in the body-fixed frame and η is the vehicle position and orientation vector in the earth-fixed frame. M is the inertia matrix, including both rigid body and added mass terms. C is the matrix of Coriolis and centripetal terms, including both rigid body and added mass terms. D is the hydrodynamic damping matrix. The vector g describes the gravitational and buoyant restoring forces. The vector

$$B = \begin{bmatrix} F_x & F_y & M_z & M_x & M_y & F_z \end{bmatrix}^T \tag{2}$$

represents the input forces and moments in the body-fixed frame, and is a linear combination of the individual thruster forces

$$T = \begin{bmatrix} T_1 & \cdots & T_n \end{bmatrix}^T \tag{3}$$

such that

$$B = AT \tag{4}$$

The transformation matrix A is entirely a function of the particular vehicle's geometry, and will be referred to as the $thruster\ configuration\ matrix$. This matrix A is generally non-square, and must ultimately be inverted [8], [9] so that the thrusters can be issued their individual commands as a function of the desired vehicle-fixed body forces. If there is redundancy in the thruster configuration, then the geometry of the system itself may be exploited to achieve fine motion control [10].

B. ODIN Geometry

ODIN is an AUV that was developed at the Autonomous Systems Laboratory of the University of Hawai'i. The vehicle has eight bi-directional thrusters (four pairs each of vertically and horizontally oriented), shown in Figure 1, which are positioned symmetrically around its spherically shaped hull, as in Figure 2.

It is a relatively small vehicle, measuring less than 1 meter in diameter, with a mass of about 150 kg. Its sealed

0-7803-8463-6/04/$20.00 ©2004 IEEE

Fig. 1. ODIN Thrusters

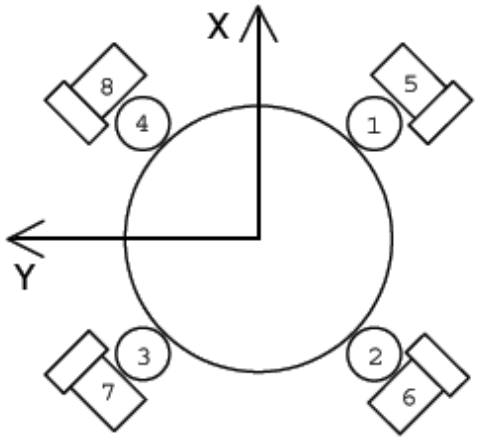

Fig. 2. ODIN Thruster Geometry

anodized aluminum hull is rated for operation to about 40 meters in depth, and is slightly positively buoyant in water. The vehicle is designed for instantaneous omni-directional motion and is an excellent platform for the efficient testing of newly developed motion control algorithms [11].

$$\begin{bmatrix} 0.7 & -0.7 & -0.7 & 0.7 & 0 & 0 & 0 & 0 \\ 0.7 & 0.7 & -0.7 & -0.7 & 0 & 0 & 0 & 0 \\ 0.5 & -0.5 & 0.5 & -0.5 & 0 & 0 & 0 & 0 \\ 0 & 0 & 0 & 0 & 0.3 & 0.3 & -0.3 & -0.3 \\ 0 & 0 & 0 & 0 & 0.3 & -0.3 & -0.3 & 0.3 \\ 0 & 0 & 0 & 0 & -1 & -1 & -1 & -1 \end{bmatrix} \quad (5)$$

The thruster configuration matrix for ODIN, shown in (5), displays the symmetry of the hardware setup. Each of the four horizontal thrusters provides equal relative thrust for the surge, sway, and yaw motions, as seen in the first three rows of the first four columns. The four vertical thrusters also have relatively equal contributions to the roll, pitch, and heave motions, as seen in the last three rows of the last four columns. It is key to note that the motions from the horizontal and vertical thrusters are completely decoupled due to the geometry of the vehicle.

C. SAUVIM Geometry

SAUVIM is under continuing development by the joint effort of Marine Autonomous Systems Engineering, Inc., the Autonomous Systems Laboratory of the University of Hawai'i, and the Naval Undersea Warfare Center, Rhode Island. It is equipped with a seven degree-of-freedom robotic manipulator and will be capable of untethered autonomous operation at 6000 meters, which is generally considered as $full\ ocean\ depth$. The vehicle is currently in its shallow-water incarnation of development, which provides for easier testing and fabrication at relatively low cost. In its current form, the vehicle is rated for operation at 1300 meter depth with aluminum pressure vessels to house the electronics, shallow-water foam, and a fiberglass fairing. The subsequent stage of development will be to pressure harden the vehicle for full ocean depth by upgrading the pressure housings to titanium, and adopting syntactic foam for flotation. In contrast to ODIN, it is a relatively large vehicle of about 6 by 2 by 2 meters in size, and a mass of about 1800 kg in shallow water form, and 3600 kg in deep water form. The geometry of the thruster setup is shown in Figure 3.

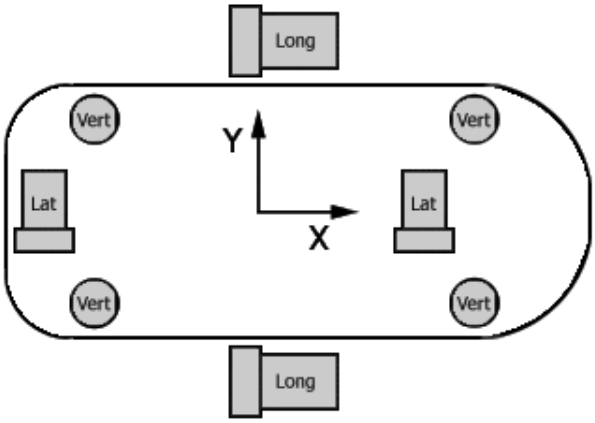

Fig. 3. SAUVIM Thruster Geometry

Fig. 4. SAUVIM Thrusters

There are many inherent asymmetries in the hardware configuration of SAUVIM. First of all, the vehicle geome-

try and the thruster arrangement is intended for motion primarily in the forward direction. Also, none of the thruster outputs are symmetrically bidirectional by design, and the two longitudinal thrusters are of a different model which provides more thrust. In application, maximum measured outputs have been on the order of 245 N in the forward direction, and 115 N in reverse for the larger, high-output thrusters. The smaller thrusters have displayed at most 110 N in the forward direction, and 40 N in reverse. These thrusters are shown in Figure 4. Furthermore, SAUVIM's center of mass is not precisely at the centroid of the vehicle, and will in fact change over time due to several factors including the deployment and motion of the robotic arm, movement of ballast for motion compensation and vehicle trim, or payload increase from sample collection or object retrieval.

$$\begin{bmatrix} 1 & 1 & 0 & 0 & 0 & 0 & 0 & 0 \\ 0 & 0 & 1 & 1 & 0 & 0 & 0 & 0 \\ -1.1 & 1.0 & 1.3 & -2 & 0 & 0 & 0 & 0 \\ 0 & 0 & 0.2 & 0.2 & 0.8 & -0.7 & 0.8 & -0.7 \\ -0.2 & -0.2 & 0 & 0 & -1.6 & -1.6 & 1.3 & 1.3 \\ 0 & 0 & 0 & 0 & 1 & 1 & 1 & 1 \end{bmatrix} \quad (6)$$

The thruster configuration matrix for SAUVIM is shown in (6). The numbers expose the lack of symmetry in the placement of the thrusters on the vehicle's frame. Also, the last three rows of the first four columns reveal the coupling between the longitudinal thrusters and pitch, as well as the coupling between the lateral thrusters and roll motion. In the study of the geometry, these off-diagonal coupling terms in the matrix are not negligible. However, a study of the vehicle's dynamics would also reveal that SAUVIM is quite stable in roll and pitch, so that these terms would be reduced. A combination of the dynamics with the geometry is important, and will be further explored in future work..

III. Implementation and Experiments

A. ODIN

Since the vehicle and the thrusters are relatively small in size, experiments could be conducted in the laboratory, with a water tank, a simple lever system, and a force sensor. Each of the eight thruster controllers for ODIN were tuned for matched outputs relative to each other. These bi-directional thrusters were designed to provide equal thrust in both the forward and reverse directions. The measured input voltage to output thrust relationship for the eight ODIN thrusters is plotted in Figure 5. The graph confirms that the thruster amplifier gains are well-tuned, relative to one another, such that the output curves are reasonably matched. Note that half of the curves have a negative slope for the reason that these propellers are counter-rotating relative to the others, which is necessary to reduce the coupling between rotational and translational motions. For each thruster, the slopes in the forward and reverse directions agree favorably, which verifies the symmetrically bi-directional design. The graph also reveals a dead zone of approximately 1.2 Volts, in which a non-zero input results in zero output. For these particular thrusters, this dead zone is primarily a result of friction in both the motor and in the radial teflon shaft seals.

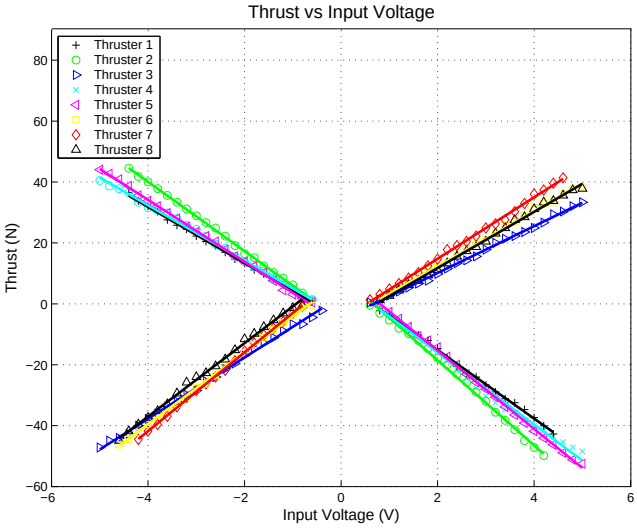

Fig. 5. Thrust vs Input Voltage for ODIN thrusters

B. SAUVIM

The SAUVIM vehicle is relatively large, so the thrusters, batteries, and controllers needed to be removed from the frame and there needed to be a sufficient volume of water for the high-output thrusters, so the experiments were conducted at the University of Hawai'i swimming pool. The test setup is shown in Figure 6, and includes the controllers/amplifiers, the lever system with force sensor, the thrusters, a 144 Volt power supply, and one 144 Volt battery bank.

The initial experiment collected the output thrust as a function of the input command voltages and is shown for the two longitudinal thrusters in Figure 7. Note that there is no thrust data between zero and 18 N due to limitations in the force sensor. A prominent feature of the the approximately linear curves is that the slopes of the functions in the forward direction is about double that of the reverse direction. The downwards and upwards facing triangles in the plot represent gain settings which were relatively small and large, respectively. The former curve verifies the command input to be $+/-10$ V, and the latter curve shows that the maximum attainable thrust is about 245 N forward, and 98 N in reverse. The next step was to tune the gains for the two thrusters, such that both reach the identical maximum output at 10 Volts. The circles and squares on the plot show the results after the tuning process. The reason that the curve for thruster 2 has a small constant shift is that there is an offset bias that is tuned slightly toward positive voltage, and could be easily corrected in the future. Note also that the maximum reverse thrust has increased from 98 N to about 115 N after the tuning process. It was observed that the thrusters draw more current in the reverse direction than in the forward direction, so thruster 2, with the large gain, was reaching

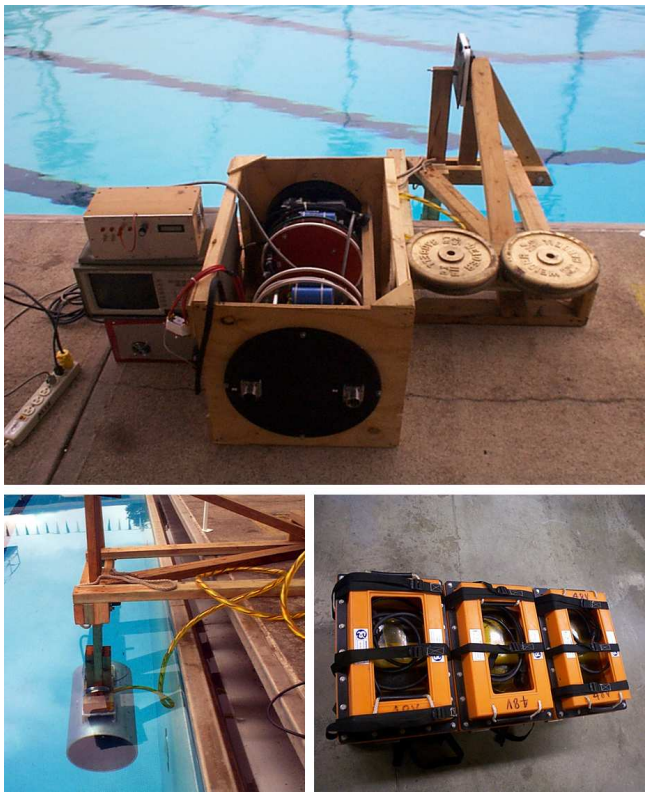

Fig. 6. SAUVIM Thruster Test Setup

the current limit before arriving at its maximum attainable output.

It is well documented that for marine thrusters, the output thrust is a function of the propeller shaft's angular velocity squared. Since the motor speed could be monitored through the built-in Hall effect sensors, then with the planetary gear ratio in account, the shaft velocities were also recorded along with the voltage and thrust information during the tests. The relationship between the shaft velocity and thrust is shown in Figure 8.

The plot shows the four test runs of the two longitudinal thrusters with two different gain settings each. It is clear that the result is independent of the selected gains, and that the experimentally derived functions accurately follow the theory. This may suggest that it may be preferable to monitor the shaft velocity as an input variable for the motion control algorithm, as opposed to the voltage. In this way, the system is less sensitive to changes in the gain settings. This is because the velocity to force relationship is only a function of mechanical hardware specifications, such as the propeller blade angle. It is the relationship between voltage and shaft velocity that depends on the electronics, and is demonstrated in Figure 9.

C. Battery Power

Since ODIN functions as an untethered vehicle, it operates on stored power. There are a total of twenty-four 12 Volt lead-acid batteries, arranged into 24 Volt pairs. Two pairs power the computer system, and the other ten pairs power the thrusters. Since SAUVIM is also designed

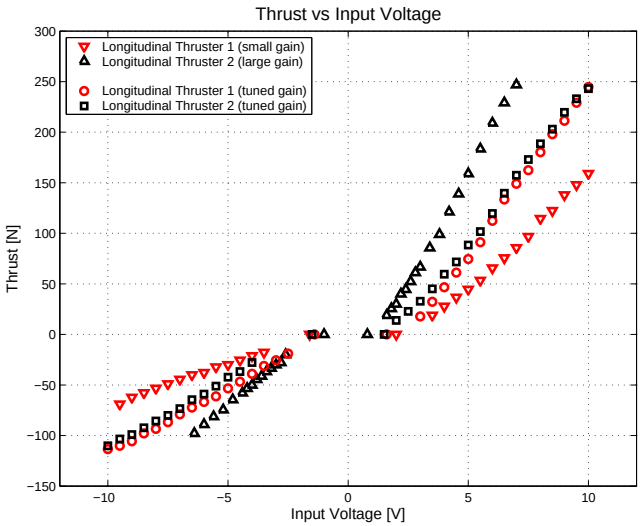

Fig. 7. Thrust vs Input Voltage for SAUVIM Logitudinal Thrusters

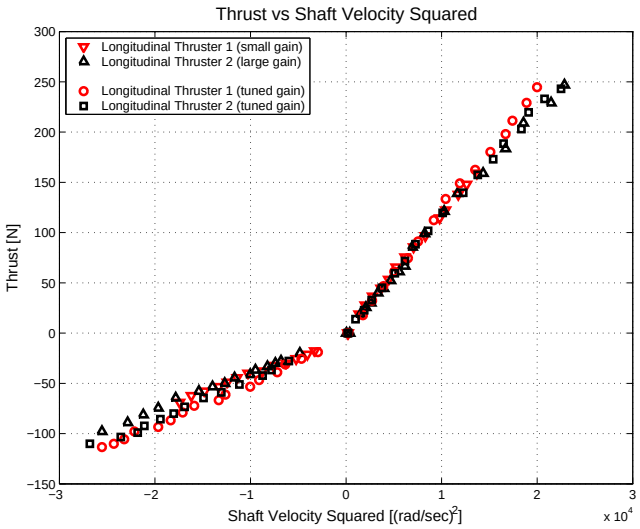

Fig. 8. Thrust vs Shaft Velocity Squared for SAUVIM Logitudinal Thrusters

for untethered operation, its power source in its current configuration consists of six 24 Volt and six 48 Volt lead-acid batteries, arranged into four banks of three, powering the six pressure vessels which house all of the electronics. The battery layout is diagramed in Figure 10. In detail, the 24 Volt and 48 Volt batteries are actually packs of two and four 12 Volt batteries respectively, connected in series and housed in oil-filled plastic containers. There are ongoing arrangements to upgrade the power source to hydrogen fuel cells for lower weight and higher energy density.

The eight thrusters are driven by two separate 144 Volt battery banks. One bank powers the two longitudinal thrusters and two of the vertical thrusters, whereas the other bank powers the two lateral thrusters and the remaining two vertical thrusters. If there is a power fault, depending on which of the battery banks go out, the vehicle is still assured power for motion both in heave translation and yaw, and also one of either surge or sway translation. In

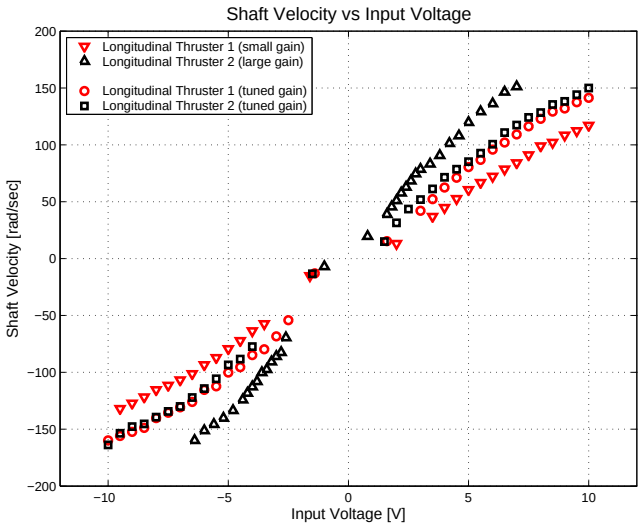

Fig. 9. Shaft Velocity vs Voltage for SAUVIM Logitudinal Thrusters

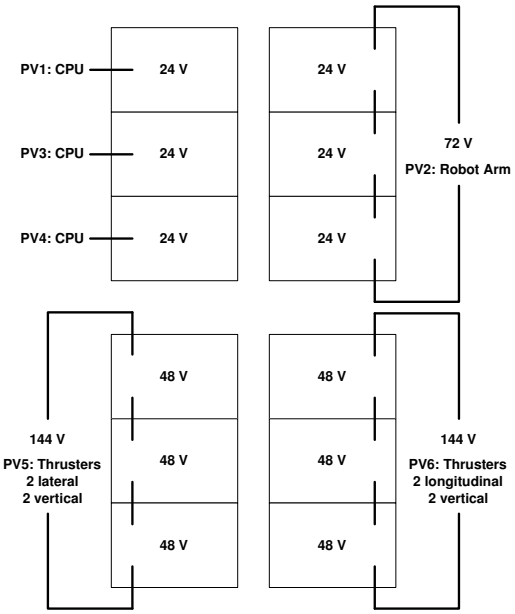

Fig. 10. Battery Layout: Distribution to Pressure Vessels 1-6 (PV 1-6)

this arrangement, the vehicle could possibly continue its mission, but should at least be able to return for retrieval.

So far, the batteries have been delivering consistent power over the span of their charge cycles. It is fortunate that the power drops off rapidly when the batteries are close to being completely discharged. Otherwise, there would be a relatively longer span of time with decreased performance and reliability. Experimentally, after some amount of data collection for the various thrusters, the batteries started to fail. The data displayed in Figure 11 captured this event in progress. A high-voltage power supply was constructed to ensure consistent power to the thrusters throughout the experiments. The plot shows the apparent difference between power sources. It is clear when the battery power started to drop off as compared to the power supply.

This data reveals the sensitivity of the voltage-to-thrust

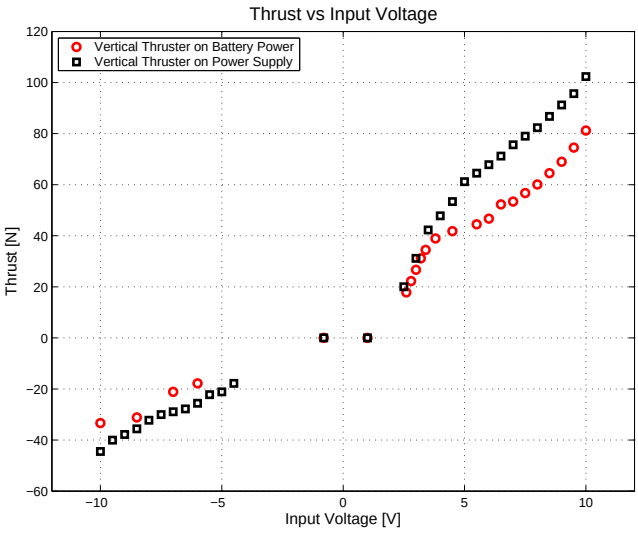

Fig. 11. Thrust vs Input Voltage for SAUVIM Vertical Thruster

curve as the power source levels change with time. The output thrust as a function of shaft velocity is shown in Figure 12, and verifies the expected model. The plot demonstrates that the mechanical configuration had been unchanged, and since both sets of data were taken with the same thruster and with the same gain settings, then the dependence must be between the input voltage and shaft speed, which is is confirmed in Figure 13. It may be preferable to monitor the shaft velocity as a control input, instead of the voltage, since it seems to be more robust to changes in the electronics such as the power delivery or the gain settings.

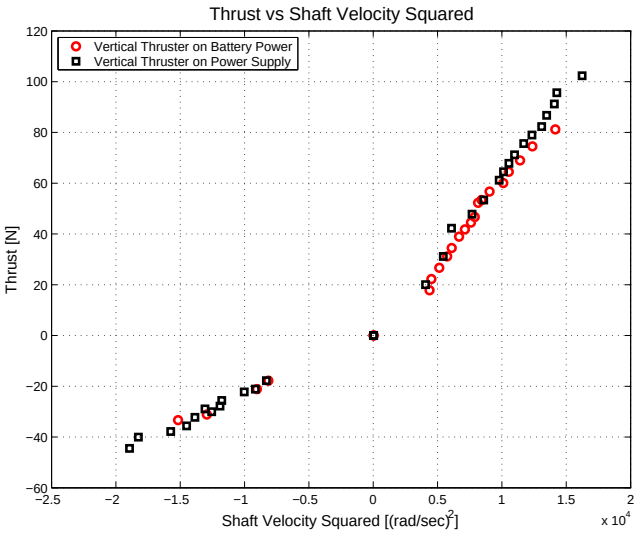

Fig. 12. Thrust vs Shaft Velocity Squared for SAUVIM Vertical Thruster

IV. Conclusion

The experience gained through this experimentation process should provide a practical guideline to improve the performance of an autonomous underwater vehicle

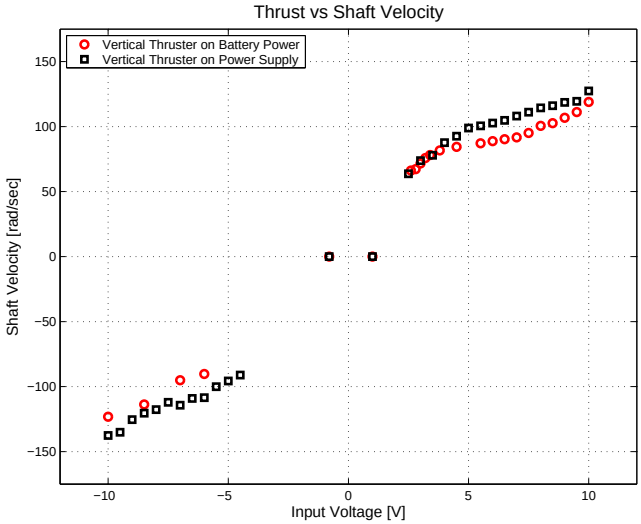

Fig. 13. Shaft Velocity vs Input Voltage for SAUVIM Vertical Thruster

designed for fine motion control applications. Important topics include the thorough understanding of the geometric configuration of the vehicle, and the effect of the thruster amplifier settings and of the power source. The experiments revealed the empirical relationship between voltage, propeller shaft velocity, and thrust, which can be modelled by a couple of polynomial approximations.

Future work can include the integration of the vehicle dynamics with the geometry to provide a complete and well-tuned vehicle model. Also, since the vehicles in this test are equipped with redundant thrusters, the systems can be further modified with a fault-tolerant scheme.

ACKNOWLEDGMENT

This research was sponsored in part by the NSF PYI Award (BES91-57896), NSF (BES97-01614, INT9603043), and ONR (N00014-97-1-0961, N00014-00-1-0629, N00014-02-1-0840).

REFERENCES

[1] A. J. Healey, S. M. Rock, S. Cody, D. Miles, and J. P. Brown, "Toward an Improved Understanding of Thruster Dynamics for Underwater Vehicles," *IEEE Journal of Oceanic Engineering*, vol. 20, no. 4, pp. 354 – 361, 1995.

[2] A. Leonessa and D. Luo, "Nonlinear identification of marine thruster dynamics," in *MTS/IEEE Conference and Exhibition OCEANS 2001*, 2001, pp. 501 – 507.

[3] L. Whitcomb and D. Yoerger, "Development, comparison, and preliminary experimental validation of nonlinear dynamic thruster models," *IEEE Journal of Oceanic Engineering*, vol. 24, 1999.

[4] D. Smallwood and L. Whitcomb, "The effect of model accuracy and thruster saturation on tracking performance of model based controllers for underwater robotic vehicles: Experimental results," in *IEEE International Conference on Robotics and Automation*, Washington, DC, 2002, pp. 1081 – 1087.

[5] S. K. Choi and J. Yuh, "Development of the Omni-Directional Intelligent Navigator," *IEEE Robotics and Automation Magazine*, vol. 2, 1995.

[6] J. Yuh and S. K. Choi, "Semi-Autonomous Underwater Vehicle for Intervention Missions (SAUVIM)," *Sea Technology*, 1999.

[7] T. I. Fossen, *Guidance and Control of Ocean Vehicles*. Chichester: John Wiley & Sons, 1994.

[8] Y. Nakamura, *Advanced Robotics Redundancy and Optimization*. Addison-Wesley, 1991.

[9] G. Strang, *Introduction to Linear Algebra*. Wellesley Cambridge Press, 1998.

[10] A. Hanai, H. T. Choi, S. K. Choi, and J. Yuh, "Minimum energy based fine motion control of underwater robots in the presence of thruster nonlinearity," in *IEEE/RSJ International Conference on Intelligent Robots and Systems*, 2003, pp. 559 – 564.

[11] H. T. Choi, A. Hanai, S. K. Choi, and J. Yuh, "Development of an underwater robot, ODIN-III," in *IEEE/RSJ International Conference on Intelligent Robots and Systems*, 2003, pp. 836 – 841.